Biomedical Research 2017; 28 (8): 3483-3486

ISSN 0970-938X
www.biomedres.info

Internal strains of anulus fibrosus in the intervertebral disc under axial compression load.

Qing Liu[1], Xiu-Ping Yang[1], Kun Li[2], Tao Yang[1], Jin-Duo Ye[1], Chun-Qiu Zhang[1*]

[1]Tianjin Key Laboratory for Advanced Mechatronic System Design and Intelligent Control, Tianjin University of Technology, Tianjin, PR China

[2]School of Electronic Information Engineering, Tianjin University of Technology, Tianjin, PR China

Abstract

In this study, the unconfined compression experiments of the intervertebral disc were conducted by applying an optimized digital image correlation (DIC) technique, and the internal strain distribution was analyzed for the disc. It was found that the anulus fibrosus (AF) radial displacement was outward in all the six test regions: inner AF, middle AF and outer AF both in anterior and posterior region. Middle AF exhibited the highest radial strains both in posterior AF and anterior AF with the increase of loads. It was noted that all samples demonstrated a nonlinear axial stress-axial strain profile in the process of deforming, and demonstrated an elastic region once the sample was deformed beyond its toe region. Inner AF exhibited the highest axial strains, while outer AF exhibited the lowest axial strains during static compressive loading. This study provides important new data in understanding the internal strain distribution, and provides a technique and baseline data for evaluating surgical treatments.

Keywords: Intervertebral disc, Anulus fibrosus, Internal strain, Axial compression, Optimized DIC technique.

Accepted on December 28, 2016

Introduction

Lumber disc herniation, which is the complete rupture of the annulus fibrosus along with extrusion of the nucleus pulposus, is commonly associated with back pain [1]. The mechanical state in the intervertebral disc is highly associated with the development of lumber disc herniation, and several motion segment studies have quantified external disc displacement and internal pressure [2]. However, limited success has been achieved when attempting to quantify mechanical behaviors within the disc. Therefore, there remains a critical need for quantitative measures of internal mechanical behavior of the disc under physiologic loading.

The intervertebral disc (IVD) is a complex strcture that transmits and distributes large loads on the spine while providing flexibility [3]. The IVD is composed of three anatomical elements [4]: the anulus fibrosus (AF), the nucleus pulposus (NP) and the endplates (EP), as shown in Figure 1a. In the last ten years, many scholars applied finite element method to study the biomechanical properties of the intervertebral disc [5,6]. However, the finite element study for internal behaviors of the intervertebral disc are difficult to validate due to lack of experimental data [7-10].

Experimental studies have attempted to measure deformations of the intervertebral disc using radiographic or optical imaging methods [11,12]. Research indicated that time, degeneration, posture, muscle tone and loading would influence the

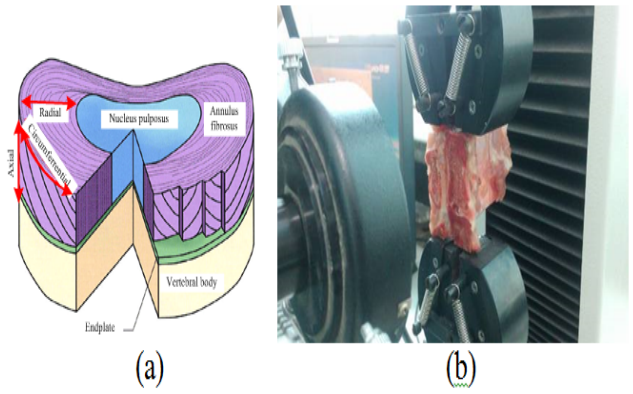

Figure 1. *Mechanical loading device for the lumbar disc under compressive load. (a) Schematic of the intervertebral disc (b) Mechanical loading device.*

mechanical state of the intervertebral disc [13-15]. Several studies have experimentally measured the internal disc deformations, and previous studies visualized internal deformations of the disc by placing metal beads in the intact disc using needles and tracking the beads on radiographs [16,17]. Heuer et al. investigate the annular fiber surface strains and disc bulging by a three-dimensional laser scanning device, then disc bulging and tissue surface strains in anuluscollagen fiber directions were computed [18,19]. O'Connell et al. measured the internal deformations and strains

of human intervertebral discs using MRI, and then qualitatively calculated the outer and inner AF radial displacement (bulge) as the average of the anterior AF and posterior AF nodal displacement at the outer and inner AF site [20,21]. Liu et al. examined the compressive and tensile responses of the intervertebral disc by applying the optimized digital image correlation technique, and calculated the internal axial strains in the disc [22].

To date, no study has quantitatively calculated the radial deformations within the disc without interruption of the structure to place markers or visualize the surfaces. The purpose of the present study is to analyse the axial and radial strains of annulus fibrosus in the intervertebral disc under compressive load. By applying the optimized digital image correlation (DIC) technique, the internal strains from six unique locations of the porcine intervertebral disk have been examined: inner AF, middle AF and outer AF both in anterior and posterior region. Simultaneously the internal strain distribution of the intervertebral disc has also been analysed.

Materials and Methods

Materials

Ten fresh porcine lumbar spine sections were obtained from 8-month-old pigs, and the L2-L3 motion segments were isolated and cut along the sagittal plane. Twenty intervertebral disc samples with vertebra were made in dimension of 30 mm in diameter and 3.5 mm in height. Previous study has confirmed geometric, anatomical, and functional similarities between porcine and human lumbar spines [23].

Experimental apparatus

A MTF-100 testing machine (Center of Mechanical Experiment in Shanghai University, China) was used to perform the compression test. The testing machine is composed of image acquisition system, mechanical loading system, computer control system and image processing software. The intervertebral disc samples were fixed in the center of the loading system by bone screws perpendicular to the disc surface, as shown in Figure 1b.

Methods

An optimized digital image correlation technique was applied to measure the two-dimensional deformation fields in the lumbar disc under unconfined compressive load. The basic principle of the optimized DIC is to automatically determine the strain field by matching the random variation of the sampling points. In this study, the metallic nano-particles were used as the marked points to reflect the deformation in different regions of the sample, and they were coated uniformly on the sample surface.

The sagittal plane of the annulus fibrous in the process of axial compression was clearly observed in the MR images (Figure 2). Figure 2c shows local region with evenly distributed nano-particles in the sagittal plane of the intervertebral disc before and after loading. A pair of marked points are chosen in this region, then the axial as well as radial strain will be determined by comparing the coordinate values between this pair of points before and after loading, using:

$$\varepsilon_z = \left(z'_{a1}z'_{a2} - z_{a1}z_{a2}\right)/z_{a1}z_{a2} \rightarrow (1)$$

$$\varepsilon_x = \left(x'_{a1}x'_{a2} - x_{a1}x_{a2}\right)/x_{a1}x_{a2} \rightarrow (2)$$

Where ε_z is the axial strain, ε_x is the radial strain. $Z_{a1}Z_{a2}$ and $Z'_{a1}Z'_{a2}$ are the Z values before and after loading. $X_{a1}X_{a2}$ and $X'_{a1}X'_{a2}$ are the X values before and after loading.

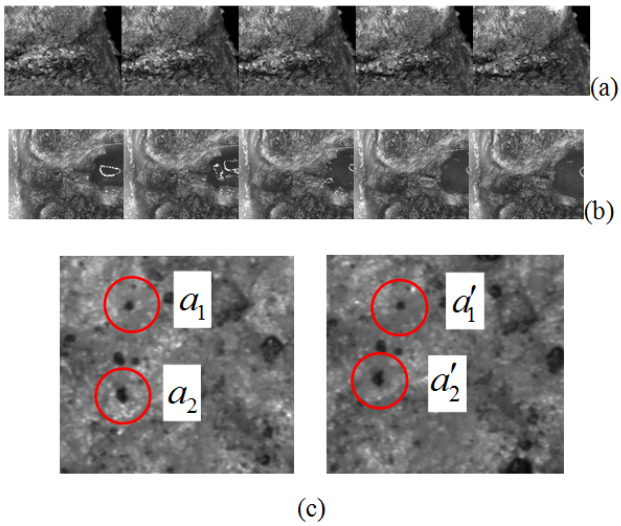

Figure 2. *Microscopic images of the intervertebral disc in the process of axial compression. (a) The sagittal plane in anterior AF (b) The sagittal plane in posterior AF (c) A section of the intervertebral disc before and after loading.*

Experimental description

Considering random error, the samples were applied continuous compressive load with the deformation rate of 1 mm/min until the strain values reached 30%. The CCD camera was focused on the sagittal plane of the samples during the whole process of loading. In addition, the loads were measured by the testing machine and were real-time displayed in the microcomputer.

Statistical analysis

A one-way analysis of variance (ANOVA) was performed to determine the statistical variances among the strain values in the compression tests. Statistical significance was considered to be significant with a P-value of <0.05. Data points used in the figures of the next section represented mean values, while the standard errors above and below mean values were indicated by error bars.

Results

The strain analysis during static loading was performed in the intervertebral disc as shown in Figure 3. Radial displacement at the mid-disc height was examined for both the anterior AF and

posterior AF to determine the magnitude and direction of AF bulging.

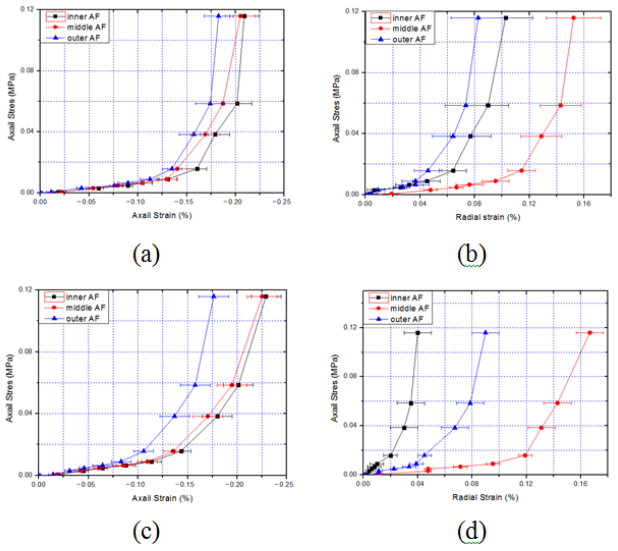

Figure 3. *Stress-strain curve of the intervertebral disc under compression load. (a) Axial stress-axial strain curve in anterior AF; (b) Axial stress-radial strain curve in anterior AF; (c) Axial stress-axial strain curve in posterior AF; (d) Axial stress-radial strain curve in posterior AF.*

For axial strain as shown in Figure 3a, the strain values at all positions increased in negative direction. The strains in the outer region were relatively lower, while the strains in the inner region were slightly greater than those in the middle region. For radial strain as shown in Figure 3b, the strain values at all positions increased in positive direction. Middle AF exhibited obviously the highest radial strains, while outer AF exhibited the lowest radial strains.

For axial strain as shown in Figure 3c, the strain values at all positions increased in negative direction, and outer AF exhibited lower axial strains than inner AF and middle AF. For radial strain as shown in Figure 3d, the strain values at all positions increased in positive direction, and middle AF exhibited higher radial strains than inner AF and outer AF. The distribution of the strains in posterior AF agreed with the experiment data in anterior AF quite well as shown in Figure 3.

Discussion

The purpose of this study was to investigate the internal strains in porcine lumbar motion segments under axial compressive load by the optimized DIC technique.

The first finding was that the anulus fibrosus radial displacement was outward in all the six test regions: inner AF, middle AF and outer AF both in anterior and posterior region, as shown in Figures 3b and 3d. The observed outward bulge of the AF was as expected based on the compression of a thick walled vessel that has been predicted in models [24]. Besides, middle AF exhibited the highest radial strains both in posterior AF and anterior AF as shown in Figures 3b and 3d. This may be due to NP shifting under applied load, the middle AF outward displacement was larger than the inner AF displacement [20,21]. Tensile radial strains are produced when the middle AF boundary deforms outward more than the inner AF, and these peak tensile strains may contribute to radial tears and herniations [25,26].

The second finding was that inner AF exhibited the highest axial strains, while outer AF exhibited the lowest axial strains during static compressive loading as shown in Figures 3a and 3c. It was in good agreement with Liu et al. [22], who found that inner AF and posterior AF experienced higher axial strains than outer AF and anterior AF. Besides, all samples demonstrated a nonlinear axial stress-axial strain profile in the process of deforming, and demonstrated an elastic region once the sample was deformed beyond its toe region as shown in Figures 3a and 3c. This result is in good agreement with early research by Causa et al. [27], who obtained the stress-strain curves by generalized compression tests.

Besides, the present study was conducted under unconfined compression. As we were not able to account for deformations in the disc that are not perpendicular to the plane of the imaging, there will be errors in the strain calculations.

Conclusions

The optimized digital image correlation technique was applied to investigate the internal strain distribution of the intervertebral disc under unconfined compression load. Firstly, the results showed that the anulus fibrosus radial displacement was outward with the increase of loads. Secondly, it was found that middle AF exhibited the highest radial strains both in posterior AF and anterior AF. Thirdly, it was noted that inner AF exhibited the highest axial strains, while outer AF exhibited the lowest axial strains during static compressive loading.

Acknowledgements

The project was partly supported by the National Natural Science Foundation of China (No. 11432016, 11372221, and 11672208) and the Natural Science Foundation of Tianjin (No. 13JCQNJC01300, 15JCYBJC19800).

References

1. Chen HL, Guo KJ, Yuan F, Ding N. Effect of stress on intervertebral disc and facet joint of novel lumbar spine soft implant: biomechanical analysis. Biomed Res Ind 2014; 25: 199-202.
2. Peloquin JM, Santare MH, Elliott DM. Advances in quantification of meniscus tensile mechanics including nonlinearity, yield, and failure. J Biomech Eng 2016; 138: 021002.
3. Brandolini N, Cristofolini L, Viceconti M. Experimental methods for the biomechanical investigation of the human spine: a review. J Mech Med Biol 2014; 14: 1430002.
4. Jacobs NT, Cortes DH, Peloquin JM, Vresilovic EJ, Elliott DM. Validation and application of an intervertebral disc finite element model utilizing independently constructed

tissue-level constitutive formulations that are nonlinear, anisotropic, and time-dependent. J Biomech 2014; 47: 2540-2546.

5. Schmidt H, Galbusera F, Rohlmann A, Shirazi-Adl A. What have we learned from finite element model studies of lumbar intervertebral discs in the past four decades? J Biomech 2013; 46: 2342-2355.
6. Du CF, Yang N, Guo JC, Huang YP, Zhang C. Biomechanical response of lumbar facet joints under follower preload: a finite element study. BMC Musculoskelet Disord 2016; 17: 1-13.
7. Yang H, Nawathe S, Fields AJ, Keaveny TM. Micromechanics of the human vertebral body for forward flexion. J Biomech 2012; 45: 2142-2148.
8. Huang J, Yan H, Jian F, Wang X, Li H. Numerical analysis of the influence of nucleus pulposus removal on the biomechanical behavior of a lumbar motion segment. Comp Meth Biomech Biomed Eng 2015; 18: 1516-1524.
9. Schmidt H, Bashkuev M, Galbusera F. Finite element study of human lumbar disc nucleus replacements. Comp Meth Biomech Biomed Eng 2014; 17: 1762-1776.
10. Schmidt H, Haeussler K, Wilke HJ. Structural behavior of human lumbar intervertebral disc under direct shear. J Appl Biomater 2015; 13: 66-71.
11. Yoder JH, Peloquin JM, Song G, Tustison NJ, Moon SM, Wright AC, Vresilovic EJ, Gee JC, Elliott DM. Internal three-dimensional strains in human intervertebral discs under axial compression quantified noninvasively by magnetic resonance imaging and image registration. J Biomech Eng 2014; 136: 111008.
12. Palanca M, Brugo TM, Cristofolini L. Use of digital image correlation to investigate the biomechanics of the vertebra. J Mech Med Biol 2015; 15: 1540004.
13. Ryan G, Pandit A, Apatsidis D. Stress distribution in the intervertebral disc correlates with strength distribution in subdiscal trabecular bone in the porcine lumbar spine. Clin Biomech 2008; 23: 859-869.
14. Little JP, Pearcy MJ, Tevelen G, Evans JH, Pettet G. The mechanical response of the ovine lumbar anulus fibrosus to uniaxial, biaxial and shear loads. J Mech Behav Biomed Mater 2010; 3: 146-157.
15. Little JP, Pearcy MJ, Izatt MT, Boom K, Labrom RD, Askin GN, Adam CJ. Understanding how axial loads on the spine influence segmental biomechanics for idiopathic scoliosis patients: A magnetic resonance imaging study. Clin Biomech 2015; 32: 220-228.
16. Seroussi RE, Krag MH, Muller DL, Pope MH. Internal deformations of intact and denucleated human lumbar discs subjected to compression, flexion, and extension loads. J Orthop Res 1989; 7:122-131.
17. Chu JY, Skrzypiec D, Pollintine P, Adams MA. Can compressive stress be measured experimentally within the anulusfibrosus of degenerated intervertebral discs. Proc Inst Mech Eng H 2008; 222: 161-170.
18. Heuer F, Schmidt H, Wilke HJ. The relation between intervertebral disc bulging and annular fiber associated strains for simple and complex loading. J Biomech 2008; 41: 1086-1094.
19. Heuer F, Wolfram U, Schmidt H, Wilke HJ. A method to obtain surface strains of soft tissues using a laser scanning device. J Biomech 2008; 41: 2402-2410.
20. O'Connell GD, Vresilovic EJ, Elliott DM. Human intervertebral disc internal strain in compression: the effect of disc region, loading position, and degeneration. J Orthop Res 2011; 29: 547-555.
21. O'Connell G, Johannessen WE, Elliott D. Human internal disc strains in axial compression measured noninvasively using magnetic resonance imaging. Spine 2007; 32; 2860-2868.
22. Liu Q, Wang TY, Yang XP, Li K, Gao LL, Zhang CQ, Guo YH. Strain distribution in the intervertebral disc under unconfined compression and tension load by the optimized digital image correlation technique. PProc Inst Mech Eng H 2014; 228: 486-493.
23. Monaco LA, Dewitteorr SJ, Gregory DE. A comparison between porcine, ovine, and bovine intervertebral disc anatomy and single lamella annulus fibrosus tensile properties. J Morphol 2015; 277: 244-251.
24. Natali AN. A hyperelastic and almost incompressible material model as an approach to intervertebral disc analysis. J Biomed Eng 1991; 13: 163-168.
25. Haefeli M, Kalberer F, Saegesser D, Nerlich AG, Boos N, Paesold G. The course of macroscopic degeneration in the human lumbar intervertebral disc. Spine 2006; 31: 1522-1531.
26. Vernonroberts B, Fazzalari NL,Manthey BA. Pathogenesis of tears of the anulus investigated by multiple-level transaxial analysis of the T12-L1 disc. Spine 1997; 22: 2641-2646.
27. Causa F, Manto L, Borzacchiello A, Santis RD, Netti PA, Ambrosio L, Nicolais L. Spatial and structural dependence of mechanical properties of porcine intervertebral disc. J Mater Sci Mater Med 2002; 13: 1277-1280.

*Correspondence to:

Chun-Qiu Zhang

School of Mechanical Engineering

Tianjin University of Technology

Tianjin

PR China